Published in final edited form as:
Bioconjug Chem. 2009 October 21; 20(10): 1992–2000. doi:10.1021/bc900302t.

Biomolecule Labeling and Imaging with a New Fluorenyl Two-Photon Fluorescent Probe

Alma R. Morales[†], **Ciceron O. Yanez**[†], **Katherine J. Schafer-Hales**[§], **Adam I. Marcus**[§], and **Kevin D. Belfield**[†,‡,*]

[†]Department of Chemistry, University of Central Florida, P.O. Box 162366, Orlando, FL 32816-2366

[§]Winship Cancer Institute, Emory University School of Medicine, Atlanta, GA 30322

[‡]CREOL, The College of Optics and Photonics, University of Central Florida, P.O. Box 162366, Orlando, FL 32816-2366

Abstract

Closely involved in the progression of nonlinear bioimaging is the development of optical probes for investigating biological function and activity. Introduction of new fluorescent compounds possessing enhanced nonlinearities are essential for advancing the utility of two-photon absorption (2PA) processes in the biological sciences. Herein, we report the synthesis of fluorene-based fluorophores tailored for multiphoton imaging, incorporating the succinimidyl ester and thioester functionality as reactive linkers for further coupling with a wide variety of biologically relevant molecules. The succinimidyl ester amine reactive probe was conjugated with the cyclic peptide RGDfK and polyclonal anti-rat IgG IgG protein. Upon conjugation, the basic molecular architecture and photophysical properties of the active 2PA chromophore remain unchanged. Conventional and two-photon fluorescence microscopy (2PFM) imaging of COS-7 and HeLa cells, incubated with either the fluorene-RGD peptide conjugate or the fluorene-IgG conjugate, was demonstrated. The fluorene-IgG conjugate was used to image cell spindles at early mitotic developmental stages.

INTRODUCTION

In recent years, enormous interest in the design, synthesis and characterization of fluorescent compounds with high two-photon absorption (2PA) cross sections has been increasing because of their recognized application in a number of multidisciplinary areas, particularly in the rapidly developing fields of multiphoton fluorescence imaging, optical data storage and switching, optical sensor protection, laser dyes, three-dimensional (3D) microfabrication, and photodynamic therapy (1–6). Multiphoton fluorescence bioimaging is one of the most promising among these applications, using fluorescent markers or intrinsic fluorescence in biological samples to gain insight into 3D cell structure.

Compared to conventional optical microscopy, two-photon excited fluorescence (2PEF) microscopy has a number of advantages; the first being the inherent 3D localization of excitation and fluorescence arising from the quadratic dependence on the input intensity. This quadratic or nonlinear dependence limits excitation to a tiny focal volume, which restricts both out-of-focus background excitation and provides intrinsic confocality since

[*]To whom all correspondence should be addressed: Department of Chemistry, University of Central Florida, P.O. Box 162366, 4000 Central Florida Blvd., Orlando, FL 32816-2366, USA, Ph: 407-823-1028, Fax: 407-823-2252, belfield@mail.ucf.edu.

only fluorophores in the plane of the focused beam will be excited. This prevents the need for a confocal aperture in front of the detector, thus maximizing the amount of light detected (7). Second, the spectral window 2PEF microscopy utilizes is the near-infrared (NIR), so the imaging depth is much greater and scattering is reduced, resulting in less photodamage and photobleaching than that caused by one-photon excited fluorescence techniques (8,9,10). In addition, higher signal-to-background ratios for fluorescence detection are possible resulting from well-separated excitation and emission wavelengths and reduced attenuation of NIR light in biological specimens relative to UV and visible wavelengths (7). To overcome depth of light penetration challenges, recently, progress has been reported in the use of luminescence upconversion using lanthanide ion-doped nanoscrystals (11). The lanthanide ion-doped nanocrystals exhibit good photostability and show reduced auotfluorescence, though spatial resolution is still an issue since the excitation replies on sequential linear absorption of two photons.

The potential of two-photon excitation (2PE) as a tool in fluorescence microscopy of biological samples cannot be realized without fluorescent probes or dyes possessing high 2PA cross sections for labeling nonfluorescent molecules, such as proteins, nucleic acids (NA), and peptides. Fluorescent dyes such as Alexa Fluor 405, ethidium bromide, 4',6-diamidine-2-phenylindole (DAPI), and Hoechst, which are widely used in fluorescence studies, have been shown to undergo 2PE fluorescence when complexed with NAs (12,13) though their 2PA cross sections are low.

Fluorescent probes with reactive groups are highly desirable since they can be conjugated with a vast number of biomolecules (14–21). Fluorene derivatives typically exhibit high fluorescence quantum yields and excellent photostability (22,23). Recently, fluorene-based bioconjugates have been reported as excellent 2PF materials, possessing high 2PA cross sections (24–28). As part of our efforts to develop high efficiency 2PA fluorene derivatives as novel fluorescent biomarkers, we found that A-π-π-π-A type compounds (where A is an electron withdrawing moiety and π represents a conjugated system of π bonds), such as 2,7-bis[4-(9,9-didecylfluoren-2-yl)vinyl]phenylbenzothiazole, exhibited reasonably high 2PA cross sections in the NIR, e.g. ~1185 GM at 800 nm (1 GM = 10^{-50} cm^4 sec $photon^{-1}$) (25,28) with near unity fluorescence quantum yield. However, this compound is rather hydrophobic, thereby limiting its applications in biological imaging.

By introducing one or two ethylene glycol moieties at the 9-position of the fluorene, the water solubility of the fluorene-based fluorescent probes can be greatly improved, facilitating the use of these dyes for cellular imaging. In addition, substitution at the fluorenyl 9-position with a succinimidyl-containing moiety provides a reactive linker for further biomolecule conjugation. Herein, we report the synthesis and comprehensive characterization of a new fluorescent probe, and a simple protocol of attaching this fluorescent label on an antibody to increase immunoassay sensitivity. In this work, goat anti-rat IgG antibody labeled with fluorene-NHS (**1**) was used to stain microtubules and mitotic cells.

EXPERIMENTAL SECTION

Materials and methods

2-(4-Vinylphenyl)benzothiazole **E** was synthesized as previously reported (25). The cyclic peptide (Ar-Gly-Asp-D-Phe-Lys) c(RGDfK) was purchased from Peptides International, Inc. Polyclonal anti-rat IgG (whole molecule) was purchased from Aldrich. All other chemicals and reagents were purchased from Aldrich or Acros Organics, and used as received unless otherwise noted. ^1H and ^{13}C NMR spectroscopic measurements were performed using Varian 500 or 300 NMR spectrometers at 500 or 300 MHz for ^1H (referenced to TMS at δ =

0.0 ppm) and 125 or 75 MHz for ^{13}C (referenced to $CDCl_3$ at δ = 77.0 ppm). Elemental analyses were performed at Atlantic Microlab, Inc., Norcross GA. High resolution mass spectrometry (HR-MS) analysis was performed in the Department of Chemistry, University of Florida, Gainesville, FL.

Synthesis of 9-(2-(2-methoxyethoxy)ethyl)-fluorene (A)—A solution of fluorene (6 g, 36.09 mmol) in dry THF (120 mL) was treated under nitrogen at −78 °C with *n*-BuLi (1.6 M in hexanes, 24 mL) over 25 min period. After addition, the temperature was allowed to rise to room temperature and stirring continued for 1 h. The mixture was then cooled to −78 °C and treated with a solution of bromo-2-(methoxy-ethoxy)ethane (4.9 mL, 36.1 mmol) in THF (30 mL). The temperature was then allowed to rise to room temperature and the mixture was stirred overnight. The yellow solution was neutralized with 5% HCl, and the THF was evaporated in vacuo. Extraction of the aqueous phase with CH_2Cl_2 yielded yellow oil. Purification was carried out by column chromatography using hexane/ethyl acetate (4:2) to give 7.45 g of colorless oil (77% yield). ^1H NMR (500 MHz, $CDCl_3$) δ: 7.75 (d, 2H, Ph-H), 7.53 (d, 2H, Ph-H), 7.37 (m, 4H, Ph-H), 4.11(t, 1H, CH), 3.5(m, 10H, CH_2O, CH_3), 2.31(q, 2H, CH_2). ^{13}C NMR (125 MHz, $CDCl_3$) δ: 147.01, 140.94, 127.03, 126.92, 124.55, 119.86, 71.94, 70.15, 68.42, 59.13 (CH_3), 44.52 (C9), 32.85 (CH_2). Anal. Calc. for $C_{18}H_{20}O_2$ (MW: 268.35): C, 80.56; H, 7.51; O, 11.92. Found: C, 80.55; H, 7.56.

Synthesis of 3-(9-(2-(2-methoxyethoxy)ethyl)-fluoren-9-yl)propanenitrile (B)—9-(2-(2-Methoxyethoxy)ethyl)-fluorene (4.44 g, 16.54 mmol) was dissolved in *p*-dioxane (28 mL) at room temperature. The solution was degassed under vacuum and nitrogen, after which it was treated with 40% aqueous solution of Triton B (0.25 mL). After addition, the mixture turned from yellow light to brown reddish color. The resulting solution was then treated with acrylonitrile over a 10 min. The reaction temperature was maintained between 30–40 °C by occasional cooling with ice-water throughout the addition period. The red solution thus obtained was then stirred at room temperature for 16 h. The reaction was neutralized with 10% HCl, followed by addition of distilled water. Extraction with CH_2Cl_2 afforded orange oil. The crude product was purified by column chromatography using hexane/ethyl acetate (3:2) as eluent to afford 4.43 g of colorless oil (83% yield). ^1H NMR (500 MHz, $CDCl_3$) δ: 7.72 (d, 2H, Ph-H), 7.41 (m, 6H, Ph-H), 3.29 (bd, 7H), 2.81 (t, 2H, CH_2), 2.45 (q, 4H, CH_2), 1.49 (t, 2H, CH_2). ^{13}C NMR (125 MHz, $CDCl_3$) δ: 146.74, 140.80, 128.07, 127.90, 122.93, 120.23, 119.60 (CN), 71.71, 69.95, 67.08, 59.01, 52.31, 39.04 (C9), 35.94, 11.76 (CH_2). Anal. Calc. for $C_{21}H_{23}NO_2$ (MW: 321.41): C, 78.47; H, 7.21; N, 4.36. Found: C, 78.37; H, 7.19; N, 4.44.

Synthesis of 3-(9-(2-(2-methoxyethoxy)ethyl)-2,7-dibromo-fluoren-9-yl)propanenitrile (C)—To a solution of 3-(9-(2-(2-methoxyethoxy)ethyl)-fluoren-9-yl)propanenitrile (4.71 g, 14.66 mmol) in propylene carbonate (31 mL) at 60 °C, N-bromosuccinimide (NBS, 7.38 g, 44.02 mmol) was added in one portion and the mixture was kept at 60 °C for 24 h. The reaction was diluted with water and extracted with CH_2Cl_2. The organic phase was washed several times with water, dried over $MgSO_4$, filtered, and concentrated under reduced pressure to give viscous brown oil. Purification was carried out by silica gel column chromatography using hexanes/ethyl acetate (3.5:1.5) as eluent to afford 4.5 g of a white solid (64% yield) mp = 92.5– 93.5 °C. ^1H NMR (500 MHz, $CDCl_3$) δ: 7.54 (m, 6H, Ph-H), 3.31 (s, 5H), 3.22 (t, 2H), 2.87 (t, 2H), 2.43 (t, 2H), 2.36 (t, 2H), 1.53 (t, 2H). ^{13}C NMR (125 MHz, $CDCl_3$) δ: 148.77, 138.75, 131.54, 126.54, 122.23, 121.66, 118.94 (CN), 71.70, 70.06, 66.79, 59.07, 52.93, 38.93 (C9), 35.53, 11.90 (CH_2). Anal. Calc. for $C_{21}H_{21}Br_2NO_2$ (M W: 479.2): C, 52.63; H, 4.42; Br, 33.35; N, 2.92; O, 6.68. Found: C, 52.50; H, 4.43; N, 2.93.

Synthesis of 3-(9-(2-(2-methoxyethoxy)ethyl)-2,7-dibromo-fluoren-9-yl)propanoic acid (D)—A mixture of 3-(9-(2-(2-methoxyethoxy)ethyl)-2,7-dibromo-fluoren-9-yl)propanenitrile (2.1 g, 4.38 mmol), ethylene glycol (100 mL), and aqueous NaOH (3M, 14 mL) was heated to reflux for 24 h. Ethylene glycol was removed under vacuum distillation producing yellow oil that was then neutralized with 10% HCl (aq) and extracted with CH_2Cl_2. The crude product was purified via column chromatography using hexanes/ethyl acetate (1:1) as eluent to afford 1.65 g of a white solid (76% yield) mp = 96–97 °C. ^{1}H NMR (500 MHz, $CDCl_3$) δ: 7.44 (m, 6H, Ph-H), 3.23 (bm, 7H, CH_2O, CH_3) 2.73 (t, 2H, CH_2), 2.31 (m, 4H, CH_2), 1.51 (t, 2H, CH_2). ^{13}C NMR (125 MHz, $CDCl_3$) δ: 178.10 (COOH), 149.94, 138.81, 131.04, 126.55, 121.90, 121.43, 71.69, 69.96, 66.92, 59.04, 52.85, 39.08 (C9), 34.50, 28.21. Anal. Calc. for $C_{21}H_{22}Br_2O_4$ (MW: 498.2): C, 50.63; H, 4.45; Br, 32.08; O, 12.85. Found: C, 50.68; H, 4.56.

Synthesis of 3-(9-(2-(2-methoxyethoxy)ethyl)-2,7-bis(4-(benzothiazol-2-yl)styryl)-fluoren-9-yl)propanoic acid (F)—3-(9-(2-(2-Methoxyethoxy)ethyl)-2,7-dibromo-fluoren-9-yl)propanoic acid (0.25 g, 0.50 mmol), 2-(4-vinylphenyl)benzothiazole (0.26 g, 1.51 mmol), $Pd(OAc)_2$ (0.04 g, 0.19 mmol), P(*o*-tolyl)$_3$ (0.10 g, 0.34 mmol) were transferred to a high pressure Schlenk tube. To this 8 mL mixture DMF/Et_3N (5:1) was added. The Schlenk tube was then sealed and stirred at 90 °C for 90 h. The mixture was cooled to room temperature and filtered. The solvent was removed under reduced pressure. The crude product was purified by column chromatography on silica gel, eluting first with hexane/THF (1:1), then hexane/ethyl acetate (1:1) as eluent to afford a yellow solid 0.28 g (70% yield) mp = 179– 180 °C. ^{1}H NMR (500 MHz, DMSO) δ: 11.95 (s, 1H, COOH), 8.08-8.04 (m, 6H, Ph-H), 7.98 (d, 2H, Ph-H), 7.84 (s, 2H, Ph-H), 7.79-7.74 (m, 6H, Ph-H), 7.59 (d, 2H, Ph-H), 7.50-7.37 (m, 4H, CH=CH, and 4H, Ph-H), 3.27 (q, 2H, CH_2O), 3.04-3.017(m, 5H, CH_2O, CH_3), 2.64 (t, 2H, CH_2O), 2.39-2.30 (m, 4H, CH_2), 1.33 (t, 2H, CH_2). ^{13}C NMR (125 MHz, $CDCl_3$) δ: 174.46 (COOH), 167.42 (Ar-C=N), 154.12, 149.95, 140.79, 140.52, 136.78, 134.90, 132.10, 128.21, 128.05, 127.78, 127.62, 127.18, 126.86, 123.35, 123.18, 122.93, 122.73, 121.61, 121.46, 121.09, 71.55, 69.62, 67.07, 58.18, 52.39, 38.86 (C9), 34.20, 28.99. HR-MS-ESI theoretical m/z $[M+H]^+$ = 811.26, found 811.26.

Synthesis of fluorene-NHS (1)—3-(9-(2-(2-Methoxyethoxy)ethyl)-2,7-bis(4-(benzothiazol-2-yl)styryl)-fluoren-9-yl)propanoic acid (0.2 g, 0.246 mmol), was dissolved in dimethylformamide (DMF) (3.5 mL) under N_2, then N-hydroxysuccinimide (0.031g, 0.27 mmol) was added to the mixture at room temperature. *N*,*N*′-Dicyclohexylcarbodiimide (DCC) (0.057 g) was added via syringe and the mixture was stirred at room temperature for 36 h. The mixture was then filtered and diluted with 3–4 volumes of ether to precipitate the dye. The solid was collected by filtration, redissolved in a minimum volume of DMF, and then reprecipitated by addition of ether. The solid was collected and dried to afford 0.2 g of a yellow solid (90% yield) mp = 217– 218 °C. ^{1}H NMR (500 MHz, $CDCl_3$) δ: 8.13 (dd, 6H, Ph-H), 7.93 (d, 2H, Ph-H), 7.72 (t, 6H, 4H, CH=CH, and 4H, Ph-H), 7.61 (s, 2H, Ph-H), 7.58 (d, 2H, Ph-H), 7.52 (t, 2H, Ph-H), 7.41 (t, 2H, Ph-H), 7.33 (m, 4H, Ph-H), 3.23 (m, 7H, OCH_2, CH_3), 2.88 (t, 2H, OCH_2), 2.76 (s, 4H, CH_2), 2.58 (m, 4H, CH_2), 1.95 (m, 2H, CH_2). ^{13}C NMR (125 MHz, $CDCl_3$) δ: 170.54 (C=O), 167.41 (Ar-C=N), 157.10, 154.17, 149.36, 140.85, 140.51, 137.07, 135.01, 132.23, 131.35, 128.26, 127.85, 127.31, 123.42, 122.97, 121.77, 71.85, 69.92, 58.76, 55.73, 52.60, 48.34, 34.23, 26.22, 25.38. HR-MS-ESI theoretical m/z $[M+H]^+$ = 908.27, found 908.28, theoretical m/z $[M+Na]^+$ = 930.26, found 930.26.

Synthesis of fluorene-RGD conjugate (2)—Cyclic peptide (Ar-Gly-Asp-$_D$-Phe-Lys) c(RGDfK) (15 mg, 0.024 mmol) was dissolved in DMSO (1.5 mL) and the pH was adjusted to 9 by adding aqueous $NaHCO_3$ (0.1 M). Fluorene-NHS (24 mg, 0.027 mmol) was added to

the reaction mixture and stirred for 22 h. The mixture was then diluted with 4 volumes of ether to precipitate the dye. The solid was collected by filtration, redissolved in a minimum volume of DMSO, and then reprecipitated by addition of ether. The solid was collected and dried to afford 32 mg of a yellow solid (94% yield) mp = 236–236.5 °C. HR-MS-ESI theoretical m/z $[M+H]^+$ = 1396.56, found 1396.54, theoretical m/z $[M+Na]^+$ = 1418.55, found 1418.52. ^{13}C NMR (125 MHz, $CDCl_3$) δ:172.63, 172.10, 171.75, 171.48, 171.10, 167.66 (Ar-C=N), 157.37, 154.37, 150.50, 141.04, 140.80, 138.98, 136.97, 135.14, 132.33, 131.60, 129.62, 128.66, 128.37, 127.92, 127.60, 127.42, 126.66, 126.21, 123.50, 123.08, 121.87, 121.20, 107.66, 71.79, 69.84, 67.30, 58.65, 55.53, 53.44, 52.81, 51.48, 49.27, 43.77, 38.94, 33.84, 31.42, 29.58, 29.01, 25.82, 25.12, 24.26, 23.69.

Synthesis of S-benzyl 3-(9-(2-(2-methoxyethoxy)ethyl)-2,7-bis(4-(benzo[d]thiazol-2-yl)styryl)-9H-fluoren-9-yl)propanethioate (3)—The reaction was performed under dry N_2 atmosphere. Benzylmercaptan (140 μL, 1.2 mmol) was slowly added to a mixture of 0.6 mL of 2.0 M $Al(CH_3)_3$ (1.2 mmol) in hexane and 2.5 mL of anhydrous CH_2Cl_2 cooled to 0 °C. The reaction mixture was allowed to warm to room temperature over 30–40 min. A 2.5 mL solution of fluorene-NHS (50 mg, 0.05 mmol) in DMF was added slowly to the reaction mixture and stirred under nitrogen for 16 h. The reaction mixture was then poured into distilled water and extracted with CH_2Cl_2. The organic phase was dried over $MgSO_4$ and concentrated by vacuum. The mixture was then filtered and diluted with 4 volumes of ether to precipitate the dye. The solid was collected by filtration, redissolved in a minimum volume of DMF, and reprecipitated by addition of ether. The solid was collected and dried to afford 28 mg of a yellow solid (70% yield) mp = 164–165 °C. ^1H NMR (500 MHz, $CDCl_3$) δ: 8.04 (t, 6H, Ph-H), 7.84 (d, 2H, Ph-H), 7.61 (q, 6H, Ph-H), 7.49 (m, 6H, Ph-H), 7.33 (t, 2H, Ph-H), 7.16 (m, 10H, Ph-H), 3.88 (s, 2H, CH_2), 3.23 (m, 7H, OCH_2, CH_3), 2.78 (t, 2H, OCH_2), 2.47(q, 4H, CH_2), 1.82 (t, 2H, CH_2). ^{13}C NMR (125 MHz, $CDCl_3$) δ: 198.72 (C=O), 167.94 (Ar-C=N), 156.94, 154.47, 149.25, 140.77, 140.26, 137.67, 136.85, 135.27, 132.84, 130.62, 139.66, 129.37, 128.99, 128.80, 128.79, 128.73, 128.21, 127.93, 127.52, 127.45, 127.30, 127.27, 127.20, 126.63, 125.44, 123.40, 121.88, 121.27, 120.65, 71.97, 70.24, 67.48, 59.27, 52.48, 49.39, 39.75, 38.51, 34.20. HR-MS-ESI theoretical m/z $[M+H]^+$ = 917.28, found 917.28, theoretical m/z $[M+Na]^+$ = 939.27, found 939.26.

Preparation of fluorene-IgG conjugate (4)—A solution of IgG (1 mg/mL) in freshly prepared $NaHCO_3$ (0.1 M, pH 9) solution was used. A stock solution of the amine-reactive probe **1** dissolved in anhydrous DMF (1.43×10^{-3} M) was freshly prepared and aliquots added dropwise into the IgG solution (0.3 mL) with gentle stirring. The concentration of the probe solution was varied such that a 1: 15, 1:10, and a 1:5 mol ratio of protein to probe was prepared to obtain the desired dye to protein molar ratios. The reaction was kept in the dark and allowed to stir at room temperature for 2 h. The reaction mixtures were purified from the unreacted dye by size exclusion chromatography column (12 cm length, Bio-Rad Econo-Pac® 10DG) equilibrated in and eluted with phosphate buffered saline (PBS, pH 7.2; Fisher). Fractions containing the IgG-fluorene bioconjugate were identified spectrophotometrically by monitoring both the protein fraction at 280 nm and the dye at 418 nm. The degree of labeling (DOL) was determinated as the ratio of moles of fluorophore to moles of protein (F/P) as previously described (30).

COS-7 cells incubated with fluorene-RGD peptide conjugate (2)—COS-7 cells were plated onto 4-well glass chamber slides. Stock solutions of fluorene-RGD peptide conjugate **2** dissolved in DMSO were prepared at concentrations of either 1 or 10 μM. Diluted solutions in complete growth medium were then freshly prepared and placed over

the cells for either a 1 or 2 h period. All cells were washed with PBS buffer (3×) and fixed using 3.7% formaldehyde solution for 5 min at room temperature.

Immunofluorescence analysis—HeLa Cells were fixed in PHEMO buffer (68 mmol/L PIPES, 25 mmol/L HEPES, 15 mmol/L EGTA, 3 mmol/L $MgCl_2$, 10% DMSO) with 3.7% formaldehyde, 0.05% glutaraldehyde, and 0.5% Triton X-100. Cells were washed in PBS buffer thrice for 5 minutes then blocked in 10% goat serum for 15 minutes. Microtubule staining was performed by incubating the cells with a primary antibody against tubulin from mouse, followed by incubating with the secondary antibody directed against mouse conjugated with amine reactive tag **1**.

One-photon spectral measurements—Linear photophysical properties of new fluorescent probes were investigated in spectroscopic grade solvents at room temperature. The steady-state absorption spectra were obtained with Agilent 8453 UV-visible spectrophotometer using 10 mm path length quartz cuvettes with dye concentrations of 1×10^{-5} M. The steady-state fluorescence spectra were measured with a PTI QuantaMaster spectrofluorimeter in 10 mm spectrofluorometric quartz cuvettes with dye concentrations of 1×10^{-6} M. All fluorescence spectra were corrected for the spectral responsivity of PTI detection system. Fluorescence quantum yields, Q, were measured for all compounds by a standard method (31), relative to Rhodamine 6G in ethanol ($Q = 0.94$) (32).

Conventional single-photon fluorescence images were obtained using an inverted microscope (Olympus IX70) equipped with a QImaging cooled CCD (Model Retiga EXi) and excitation mercury lamp 100 W. In order to improve the fluorescence background-to-image ratios a customized filter cube (Ex 377/50, DM 409, Em 460/50) was used for the one-photon fluorescence images. The specifications of the filter cube were tailored to match the excitation wavelength of compounds **2** and **4**, and to capture most of its emission profile.

Two-photon absorption and imaging measurements—2PA spectra of **1** were determined over a broad spectral region via a typical two-photon induced fluorescence (2PF) method relative to Rhodamine B in methanol and Fluorescein in water (pH=11) as a standards (33,34). A PTI QuantaMaster spectrofluorimeter and femtosecond Clark-MXR CPA-2010 laser that pumped an optical parametric generator/amplifier (TOPAS, Light Conversion), with pulse duration, ≈140 fs, (FWHM), tuning range 580–940 nm, pulse energies ≤ 0.15 μJ, and 1 kHz repetition rate were used. Two-photon fluorescence measurements were performed in 10 mm fluorometric quartz cuvettes with dye concentrations of 3×10^{-5} M in DMSO. The quadratic dependence of two-photon induced fluorescence intensity on the excitation power was confirmed for each excitation wavelength.

Two-photon fluorescence microscopic images were obtained with a modified Olympus Fluoview FV300 microscope system combined with a tunable Coherent Mira 900F Ti:sapphire laser. The femtosecond NIR laser beam (with 220 fs pulse width and 76 MHz repetition rate) was tuned to 730 nm and used as two-photon excitation source. The two-photon induced fluorescence intensity was collected by a 60x microscopic objective (UPLANSAPO 60×, NA= 1.35, Olympus). A high transmittance (>95%) short-pass filter (cutoff 685 nm, Semrock) was placed in front of the PMT detector of the FV300 scan head in order to filter off background radiation from the laser source (730 nm).

RESULTS AND DISCUSSION

Synthesis and characterization of the fluorenyl probes

Our previous results with 2PA fluorene-based dyes (22–28), encouraged us to further investigate this class of chromophores as two-photon excitable labels. Herein, we report the synthesis of novel two-photon excitable fluorescent labeling reagents, specifically designed to be used for molecular labeling. The symmetric hydrophobic compound 2,7-bis[4-(9,9-didecylfluoren-2-yl)vinyl]phenylbenzothiazole, an A-π-π-π-A archetype, is comprised of a rather promising chromophore and exhibited a 2PA cross-section of ca. 1185 GM at 800 nm. Thus, we decided to design an amine reactive probe based on the same chemical structure of this chromophore.

Scheme 1 depicts the design of the amine reactive probe (**1**) and shows our straightforward strategy to incorporate the succinimidyl functionality as a reactive linker on the fluorenyl 9-position for further linkage with peptides, antibody, or label a wide variety of biologically significant molecules. Synthesis of the reactive probe began with the monoalkylation of fluorene upon treatment with *n*-butyl lithium and 1-bromo-2-(2-methoxy-ethoxy)ethane in dry THF at −78 °C under nitrogen atmosphere. The product was purified via silica gel column chromatography to afford 9-[2-(2-methoxy-ethoxy)-ethyl]-fluorene (**A**) in 70% yield. The condensation of acrylonitrile in the presence of benzyltrimethylammonium hydroxide (“Triton B”) as a catalyst with intermediate **A** via Michael addition reaction provided 3-{9-[2-(2-methoxy-ethoxy)-ethyl]-fluoren-9-yl}-propionitrile (**B**). Bromination of (**B**) with NBS in propylene carbonate produced intermediate (**C**) in 60% yield. The nitrile intermediate (**C**) was hydrolyzed with NaOH in ethylene glycol to afford 3-{2,7-dibromo-9-[2-(2-methoxy-ethoxy)-ethyl]-fluoren-9-yl}-propionic acid (**D**). 3-{2,7-Bis-[2-(4-benzothiazol-2-yl-phenyl)-vinyl]-9-[2-(2-methoxy-ethoxy)-ethyl]-fluoren-9-yl}-propionicacid (**F**) was prepared via efficient Pd-catalyzed Heck coupling reaction of **D** with 2-(4-vinylphenyl)benzothiazole (**E**) in 70% yield. Esterification reaction of intermediate **G** with *N*-hydroxisuccinimide was carried out in the presence of 1,3-dicyclohexylcarbodiimide (DCC), affording the succinimidyl amine reactive probe **1** in high yield (90%) as shown in Scheme 1.

The utility of the activated ester was demonstrated by coupling chromophore **1** with RGDfK. Conjugation reaction of amine reactive probe **1** with commercial cyclopeptide (Ar-Gly-Asp-D-Phe-Lys) c(RGDfK) was carried out in DMSO at room temperature for 22 h, affording fluorene-RGD peptide conjugate (**2**) in high yield (Scheme 2). A similar protocol to the one described by Schuler *et al*. (35) was followed for the synthesis of the fluorene thioester probe (**3**), with slight modifications for the isolation and purification due to the specific properties of our probe (Scheme 3). This further demonstrates the versatility of amine-reactive probe **1** as it can readily be converted to the thiol-reactive probe (**3**). All compounds were fully characterized by NMR and elemental analysis or HR-MS.

Labeling of IgG

The use of specific antibodies labeled with fluorescent dyes to localize substances in tissues was first devised by A. H. Coons and associates (36). At first, the specific antibody itself was labeled and applied to the tissue section to identify the antigenic sites. Later, a more sensitive and versatile indirect method (37) was introduced. The primary, unlabeled, antibody is applied to the tissue section, and the excess is washed off with buffer. A second, labeled antibody from another species, raised against the IgG of the animal donating the first antibody, is then applied. The primary antigenic site is thus revealed.

A major advantage of the indirect method is enhanced sensitivity. In addition, a labeled secondary antibody can be used to locate any number of primary antibodies raised in the

same animal species without the necessity of labeling each primary antibody. There are many fluorophores used in labeling, including coumarin derivatives, phycobiliproteins, fluorescein and rhodamine. The isothiocyanate derivatives of fluorescein and rhodamine are widely used to label antibodies. In addition, the newly introduced Alexa fluorochromes are a series of fluorescent dyes with excitation/emission spectra similar to that of commonly used probes under single-photon excitation (38,39). We previously reported the results of the conjugation of certain fluorene-based fluorophores with bovine serum albumin (BSA, fraction V) and Reelin (40,41). BSA is an inexpensive commercially available protein, while Reelin is a large extracellular matrix glycoprotein, important in guiding neural stem cells in the central nervous system in normal development (42,43).

Performance of the amine reactive probe **1** was studied by labeling of polyclonal anti-rat IgG. The conjugation of succidimidyl ester probe **1** with IgG was carried out according to standard methods (30). The fluorene-IgG conjugates were separated from unbound succidimidyl ester by gel filtration chromatography in saline phosphate buffer solution (PBS, pH 7.2). The conjugation did not lead to the quenching of the fluorescence signal of the succidimidyl ester. Thus, a series of experiments were carried out in order to evaluate: 1) the maximum succinimidyl dye to protein molar ratio that can be attained without protein precipitation; 2) the optimum reaction time; and 3) the optical stability of the bioconjugate. The labeling degrees were determined spectrophotometrically. With succinimidyl derivative **1**, a degree of labeling of 3 and 6 fluorophores per IgG were obtained after a few hours of mixing the solutions containing the succinimidyl dye and the IgG, without precipitation of the conjugate. The intensities of the emission spectrum of the conjugates indicated that the signal intensity increased as the succinimidyl dye/protein molar ratio increased.

The normalized UV-visible absorption and steady-state fluorescence emission spectra of amine-reactive probe **1** and fluorene-IgG conjugate **4** in PBS (buffer pH 7.2) are shown in Figure 3. The fluorene-IgG conjugate exhibited absorption peaks corresponding to that of the IgG protein in the shorter wavelength range (λ_{max} = 280 nm) as well as that of the fluorescent dye in the longer absorption range (λ_{max} = 416 and 447 nm), and exhibited an emission maximum at 445 nm (characteristic of the fluorenyl moiety). The absorption spectrum of the fluorene-IgG conjugate **4** showed only slight broadening compared to the absorption spectrum of the unbound fluorophore **1**.

Optical properties of fluorescent markers

The RGD peptide substituent on the 9-position is not part of the chromophore's π-conjugated system of **1**, thus, there is no significant alteration of the photophysical properties of fluorene-RGD peptide conjugate **2** relative to succinimidyl amine reactive probe **1**. The absorbance maximum was observed at 413 nm for both derivatives with an emission maximum at 485 nm in DMSO. The fluorescence quantum yield (0.68) was nearly unaltered in fluorene-RGD peptide conjugate **2** (Figure 1). Additionally, no significant differences of the fluorene thioester **3** compared to the succinimidyl ester **1** were detected. The absorbance maximum was at 413 nm for both derivatives and the fluorescence quantum yield (0.69) remained practically unaltered for the thioester (Figure 2).

2PA cross sections (δ) were obtained by the up-conversion fluorescence method using a femtosecond Ti:sapphire laser as excitation source (33,34). The uncertainty in the experimental δ values is estimated to be ± 15%. The 2PA cross section measurements of symmetrical amine-reactive probe **1** and carboxylic intermediate **F** were performed in DMSO (1.6×10^{-3} M). Although, the symmetric fluorene derivatives **1** and **F** are not strictly centrosymmetric systems, they exhibit the same parity selection rules associated with centrosymmetric systems. As indicated in Figure 4, amine-reactive probe **1** and intermediate **F** show small 2PA into the first excited state, identified by the peak in the linear absorption

spectrum located approximately at 415 nm (250 GM at 830 nm). This is expected given the symmetric structure of the A–π–π–π–A molecules **1** and **F**. The second 2PA peak at ~370 nm is two-photon allowed state and exhibited a substantially higher 2PA cross section of ~1000–1100 GM at 740 nm (Figure 4).

Single- and two-photon fluorescence and cell imaging

The ability of fluorene-RGD peptide conjugate **2** to be uptaken into cells was examined using COS-7 cells (Figures 5a to 5d). Cells were incubated with a solution of 10 μM DMSO solution of chromophore **2** and, after 1 and 5 h incubation times, images were taken with a modified Olympus Fluoview FV300 microscope system. Strong fluorescence was observed after 5 h of incubation, with a homogeneous coloration of the cytoplasmic region. Differential interference contrast (DIC) and conventional (one-photon) fluorescence microscopic images of the stained cells are shown in Figures 5a and 5b. Two-photon fluorescence microscopy (2PFM) images of the fluorene-RGD peptide conjugate **2** containing cells were collected on using a modified Olympus Fluoview FV300 microscope system coupled to a tunable Coherent Mira 900F Ti:sapphire laser. Two-photon induced fluorescence was observed predominantly from the cytoplasmic region, consistent with the images collected via one-photon fluorescence imaging (Figure 5c). 3D reconstruction from overlaid upconverted fluorescence images from the complete field is shown in Figure 5d.

Having confirmed the cellular uptake of the fluorescent probes, the fluorene-IgG conjugate was investigated and compared with the analogous Alexa 488 conjugate, known for its efficiency in microtubule staining. Amine-reactive dye **1** was conjugated on a secondary antibody (Anti-rat IgG). The images were acquired via confocal microscopy and shown in Figure 6, panels a–c. Imaging results with the fluorene-IgG conjugate were reproducible and in accordance with images using the Alexa Fluor 488 conjugate. Figure 6b visibly shows the localization of microtubules labeled with the bioconjugate. The fluorescence intensity of microtubules labeled with fluorene-IgG conjugate was comparable to that of Alexa Fluor 488, with the fluorene-based probe possessing both higher two-photon absorptivity and increased photostability.

Mitosis, the process by which identical copies of the replicated genome are distributed to the daughter cells at each cell division, depends on the action of a bipolar protein machine - the mitotic spindle. The action of mitotic spindles is crucial for the formation, maintenance, and reproduction of healthy organisms. Consequently, the morphology and dynamics of zygote spindles during the mitotic process contains abundant biological information (44,45). Here, labeling microtubules with amine reactive probe **1**, conjugated with the anti-rat IgG antibody, facilitated acquiring images of spindles by confocal fluorescence microscopy at different stages of mitosis (Figure 7). Application of fluorene-IgG conjugate for investigating the ultrastructure of cells and tissues by one-photon and two-photon fluorescence microscopy greatly expands the possibilities for localization of antigens. In addition, a wide variety of fluorene conjugates of immunoglobulins of different specificities or of a variety of other proteins can be prepared. Further, this method offers new possibilities to perform double labeling experiments with two antibodies at the ultrastructural level.

The high selectivity that this fluorene-IgG conjugate exhibited for microtubules may lead to interesting applications, e.g., cytometric assays for mitosis where co-staining wouldn’t be necessary. Simply recording the image with different exposure times may allow calculation of the average number of cells that are undergoing mitosis. In the case of Figure 8, a cell count can easily be made (Figure 8b and 8e) using longer exposure times (350 ms) and an intermediate fluorescence intensity threshold (shown in Figure 8e in light blue) to account for the overall number of cells by the fluorescence signal of their nuclei. Subsequently, a

higher fluorescence intensity threshold can be set and, after recording the image with a shorter exposure time (25 ms, Figure 8d), mitotic cells can be accounted for based on this threshold (shown in green). In this particular example, if this picture represented the entirety of the cell population, two of the 20 cells (10%) would be undergoing mitosis. In addition, a higher fluorescence intensity signal for different stages of the mitotic process (anaphase, metaphase, and cytokinesis) was observed and comparable relative fluorescence intensity signals were observed.

CONCLUSIONS

Probe **1** is a promising new candidate as a contrast agent for multiphoton fluorescence imaging, partciularly considering its high fluorescence quantum yield, high photostability, and suitably high two-photon absoprtivity in the NIR. An immunolabeling procedure employing this amine reactive probe demonstrated sensitivity and versatility of amine reactive probe **1**. In combination with efficient synthesis and availability of antibodies, this protocol represents a widely applicable procedure that offers a good alternative to traditionally used methods. Experimental results demonstrated the validity of the fluorene-IgG conjugate as an effective probe to image cell spindles at early mitotic developmental stages. The intrinsically less invasive physical character of two-photon excitation for biological imaging, coupled with stable, efficient 2PA probes, provides a powerful tool for studying such sensitive systems.

Acknowledgments

The authors wish to acknowledge support from the National Institutes of Health (1 R15 EB008858-01), the U.S. Civilian Research and Development Foundation (UKB2-2923-KV-07), and the National Science Foundation (CHE-0832622).

LITERATURE CITED

1. Bhawalkar JD, He GS, Prasad PN. Nonlinear multiphoton processes in organic and polymeric materials. Rep. Prog. Phys 1996;59:1041–1070.
2. Reinhardt BA, Brott LL, Clarson SJ, Dillard AG, Bhatt JC, Kannan R, Yuan L, He GS, Prasad PN. Highly active tw o photon dyes: design, synthesis, and characterization toward application. Chem. Mater 1998;10:1863–1874.
3. Wu L-Z, Tang X-J, Jiang M-H, Tung C-H. Two-photon induced fluorescence of novel dyes. Chem. Phys. Lett 1999;315:379–382.
4. Fakis M, Polyzos J, Tsigaridas G, Parthenios J, Fragos A, Giannetas V, Persephonis P, Mikroyannidis J. Novel class of pyrylium dyes with high efficiency in lasing and two-photon absorption fluorescence. Chem. Phys. Lett 2000;323:111–116.
5. Wang HZ, Lei H, Wei ZC, Zhao FL, Zheng XG, Hu NS, Wang XM, Ren Y, Tian YP, Fang Q, Jiang MH. Spectral properties aaand effective upconverted lasing of new organic molecules. Chem. Phys. Lett 2000;324:349–353.
6. Ehrlich JE, Wu XL, Lee LYS, Hu ZY, Rockel H, Marder SR, Perry JW. Two-photon absorption and broadband optical limiting with bis-donor stilbenes. Opt. Lett 1997;22:1843–1845. [PubMed: 18188382]
7. So PTC, Dong CY, Master BR, Berland KM. Two photon excitation fluorescence microscopy. Annu. Rev. Biomed. Eng 2000;2:399–429. [PubMed: 11701518]
8. Helmchen F, Denk W. Deep tissue two-photon microscopy. Nat. Methods 2005;2:932–940. [PubMed: 16299478]
9. Zipfel WR, Williams RM, Webb WW. Nonlinear magic: multiphoton microscopy in the biosciences. Nat. Biotechnol 2003;21:1369–1377. [PubMed: 14595365]
10. Diaspro, A.; Shepard, CJR. Two-Photon Microscopy: Basic Principles and Architectures. New York: Wiley & Sons; 2002.

11. Wang F, Liu X. Recent advances in the chemistry of lanthanide-doped upconversion nanocrystals. Chem. Soc. Rev 2009;38:976–989. [PubMed: 19421576]
12. Gryczynski I, Malak H, Lakowicz JR. Multiphotn excitation of the DNA stains DAPI and Hoechst. Bioimaging 1996;4:138–148.
13. Malak H, Castellano FN, Gryczynski I, Lakowicz JR. Two-photon excitation of ethidium bromide labeled DNA. Biophys. Chem 1997;67:35–41. [PubMed: 9397517]
14. Hayek A, Bolze FE, Nicoud J-F, Duperray A, Grichine A, Baldeck PL, Vial J-C. Two-photon water-soluble dyes and their amine-reactive derivative for two-photon bio-imaging applications. Nonlinear Opt. Quant. Opt 2006;35:155–164.
15. Konecsni T, Kilar F. Monitoring of the conjugation reaction between human serum transferrin and fluorescein isothiocyanate by capillary electrophoresis. J. Chromatogr. A 2004;1051:135–139. [PubMed: 15532565]
16. Barbarella G. Oligothiophene isothiocyanates as fluorescent markers. Chem. Eur. J 2002;8:5072–5077.
17. Meltola NJ, Wahlroos R, Soini AE. Hydrophilic labeling reagents of dipyrrylmethene-BF2 dyes for two-photon excited fluorometry: syntheses and photophysical characterization. J. Fluoresc 2004;14:635–647. [PubMed: 15617270]
18. Meltola NJ, Soini AE, Hanninen PE. Syntheses of novel dipyrrylmethene-BF2 dyes and their performance as labels in two-photon excited fluoroimmunoassay. J. Fluoresc 2004;14:129–138. [PubMed: 15615038]
19. Hayek A, Ercelen S, Zhang X, Bolze F, Nicoud J-F, Schaub E, Baldeck PL, Mély Y. Conjugation of a new two-photon fluorophore to poly(ethylenimine) for gene delivery imaging. Bioconjugate Chem 2007;18:844–851.
20. Hayek A, Bolze FE, Nicoud J-F, Duperray A, Grichine A, Baldeck PL, Vial J-C. Two-photon water-soluble dyes and their amine-reactive derivative for two-photon bio-imaging applications. Nonlinear Opt. Quant. Opt 2006;25:155–164.
21. Lartia R, Allain C, Bordeau G, Schmidt F, Fiorini-Debuisschert C, Charra F, Teulade-Fichou M-P. Synthetic Strategies to Derivatizable Triphenylamines Displaying High Two-Photon Absorption. J. Org. Chem 2008;5:1732–1744. [PubMed: 18247488]
22. Belfield KD, Bondar MV, Przhonska OV, Schafer KJ. Photostability of a series of two-photon absorbing fluorene derivatives. J. Photochem. Photobiol. A: Chem 2004;162:489–496.
23. Belfield KD, Bondar MV, Przhonska OV, Schafer KJ. Photochemical properties of (7-benzothiazol-2-yl-9,9-didecylfluoren-2-yl)diphenylamine under one- and two-photon excitation. J. Photochem. Photobiol. A: Chem 2004;162:569–574.
24. Belfield KD, Schafer KJ, Mourad W, Reinhardt BA. Synthesis of new two-photon absorbing fluorene derivatives via Cu-mediated Ullmann condensations. J. Org. Chem 2000;65:4475–4481. [PubMed: 10959847]
25. Belfield KD, Morales AR, Hales JM, Hagan DJ, Van Stryland EW, Chapela VM, Percino J. Linear and two-photon photophysical properties of a series of symmetrical diphenylaminofluorenes. Chem. Mater 2004;16:2267–2273.
26. Belfield KD, Morales AR, Kang B-S, Hales JM, Hagan DJ, Van Stryland EW, Chapela VM, Percino J. Synthesis, Characterization, and Optical Properties of New Two-Photon-Absorbing Fluorene Derivatives. Chem. Mater 2004;16:4634–4641.
27. Morales AR, Belfield KD, Hales JM, Hagan DJ, Van Stryland EW. Synthesis of Two-Photon Absorbing Unsymmetrical Fluorenyl-Based Chromophores. Chem. Mater 2006;18:4972–4980.
28. Yao S, Belfield KD. Synthesis of two-photon absorbing unsymmetrical branched chromophores through direct tris(bromomethylation) of fluorene. J. Org. Chem 2005;70:5126–5132. [PubMed: 15960514]
29. Corredor CC, Huang Z-L, Belfield KD. Two-photon 3D optical data storage via fluorescence modulation of an efficient fluorene dye by a photochromic diarylethene. Adv. Mater 2006;18:2910–2914.
30. Haugland, RP. Chapter 22. In: Davis, WC., editor. Methods in Molecular Biology: Monoclonal Antibody Protocols. New Jersey: Humana Press; 1995. p. 205-215.

31. Lakowicz, JR. Principles of Fluorescence Spectroscopy. New York: Kluwer Academic/Plenum; 1999. p. 52-53.298–300, and 648
32. Fischer M, Georges J. Fluorescence quantum yield of Rhodamine 6G in ethanol as a function of concentration using thermal lens spectrometry. Chem. Phys. Lett 1996;260:115–118.
33. Xu C, Webb WW. Measurement of two-photon excitation cross sections of molecular fluorophores with data from 690 to 1050 nm. J. Opt. Soc. Am. B 1996;13:481–491.
34. Albota MA, Xu C, Webb WW. Two-photon fluorescence excitation cross section of biomolecular probes from 690 to 960 nm. Appl. Opt 1998;37:7352–7356. [PubMed: 18301569]
35. Schuler B, Pannell LK. Specific labeling of polypeptides at amino-terminal cysteine residues using Cy5-benzyl thioester. Bioconjugate Chem 2002;13:1039–1043.
36. Coons AH, Creech HJ, Jones RN. Immunological properties of an antibody containing a fluorescent group. Proc. Soc. Exp. Biol. Med 1941;47:200–202.
37. Coons AH, Leduc EH, Connolly JM. Studies on antibody production I. A method for the histochemical demonstration of specific antibody and its application to a study of the hyperimmune rabbit. J. Exp. Med 1955;102:49–60. [PubMed: 14392240]
38. Panchuk-Voloshina N, Haugland RP, Bishop-Stewart J, Bhalgat MK, Millard PJ, Mao F, Leung WY, Haugland RP. Alexa dyes, a series of new fluorescent dyes that yield exceptionally bright, photostable conjugates. J. Histochem. Cytochem 1999;47:1179–1188. [PubMed: 10449539]
39. Waterman-Storer C, Duey DY, Weber KL, Keech J, Cheney RE, Salmon ED, Bement WM. Microtubules remodel actomyosin networks in Xenopus egg extracts via two mechanisms of F-actin transport. J. Cell Biol 2000;150:361–376. [PubMed: 10908578]
40. Schafer-Hales KJ, Belfield KD, Yao S, Frederiksen PK, Hales JM, Kolattukudy PE. Fluorene-based fluorescent probes with high two-photon action cross-sections for biological multiphoton imaging applications. J. Biomed. Opt 2005;10:051402/1–051402/8. [PubMed: 16292939]
41. Morales AR, Schafer-Hales KJ, Marcus AI, Belfield KD. Amine-Reactive Fluorene Probes: Synthesis, Optical Characterization, Bioconjugation, and Two-Photon Fluorescence Imaging. Bioconjugate Chem 2008;19:2559–2567.
42. Dulabon L, Olson EC, Taglienti MG, Eisenhuth S, McGrath B, Walsh CA, Kreidberg JA, Anton ES. Reelin binds alpha3beta1 integrin and inhibits neuronal migration. Neuron 2000;27:33–44. [PubMed: 10939329]
43. Costa E, Davis J, Grayson DR, Guidotti A, Pappas GD, Pesold C. Dendritic spine hypoplasticity and down regulation of reelin and GABAergic tone in schizophrenia vulnerability. Neurobiol. Dis 2001;8:723–742. [PubMed: 11592844]
44. Kwon M, Scholey JM. Spindle mechanics and dynamics during mitosis in Drosophila. Trends Cell Biol 2004;14:194–205. [PubMed: 15066637]
45. Kline-Smith SL, Walczak CE. Mitotic spindle assembly and chromosome segregation: Refocusing on microtubule dynamics. Mol. Cell 2004;15:317–327. [PubMed: 15304213]

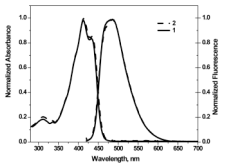

Figure 1.

Normalized UV-visible absorbance and fluorescence emission spectra of amine-reactive tag **1** (—) Qy = 0.68, and fluorene-RGD peptide conjugate **2** (---) in DMSO λ_{max}^{abs} = 413 nm; λ_{max}^{em}= 485 nm; Qy = 0.69.

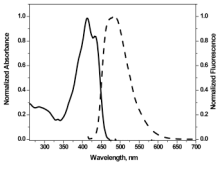

Figure 2.
Normalized UV-visible absorbance (—) and fluorescence emission (---) spectra of thioester probe **3** in DMSO λ_{max}^{abs} = 413 nm; λ_{max}^{em}= 485 nm; Qy = 0.67.

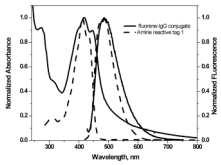

Figure 3.
Normalized absorption spectra and steady state fluorescence emission spectrum of amine-reactive tag **1** (---) and fluorene-IgG conjugate (—) in PBS buffer.

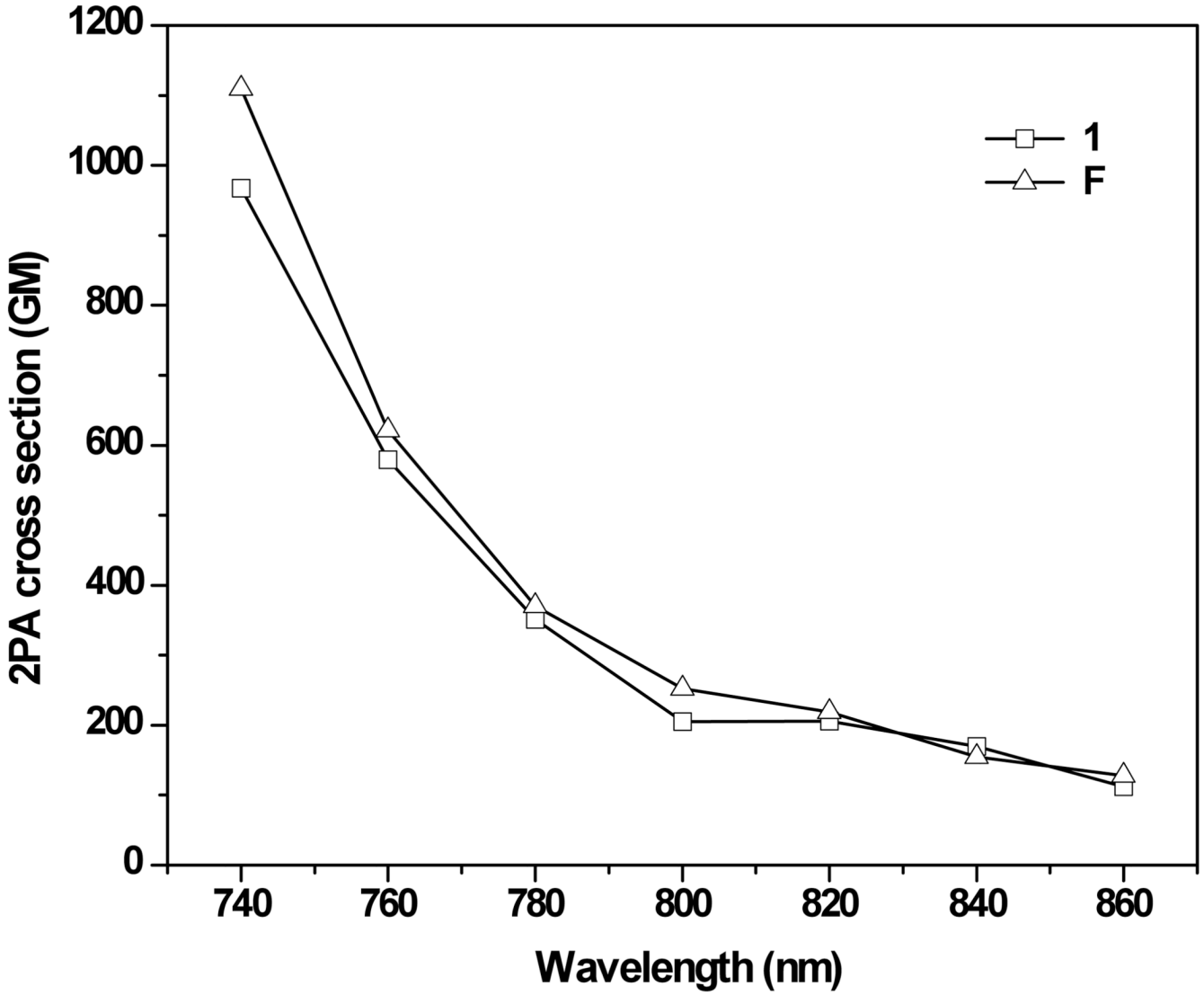

Figure 4.
2PA cross section values of carboxylic acid **F** and amine reactive tag **1** in DMSO, measured by the 2PF method using fluorescein at pH =11 as reference.

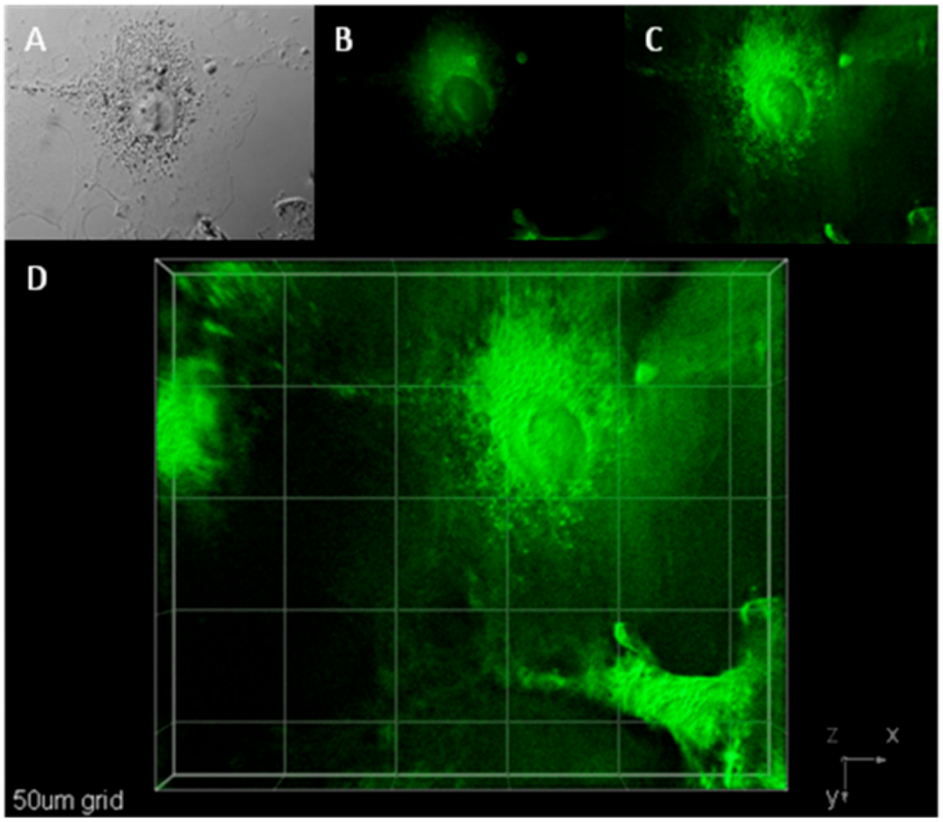

Figure 5.
COS-7 cells in PBS media, incubated for 1 h with the fluorene-RGD peptide conjugate **2** from a 10 μM solution in DMSO; UPlanSApo, N.A.=1.35, 60× oil immersion. A) DIC, 34 ms; B) one-photon fluorescence (Ex: 377/50-DM:409-Em: 525/40), 755 ms; C) two-photon upconverted fluorescence, overlay of all planes, 730 nm; D) 3D reconstruction from overlaid upconverted fluorescence images from complete field, 50 μm grid.

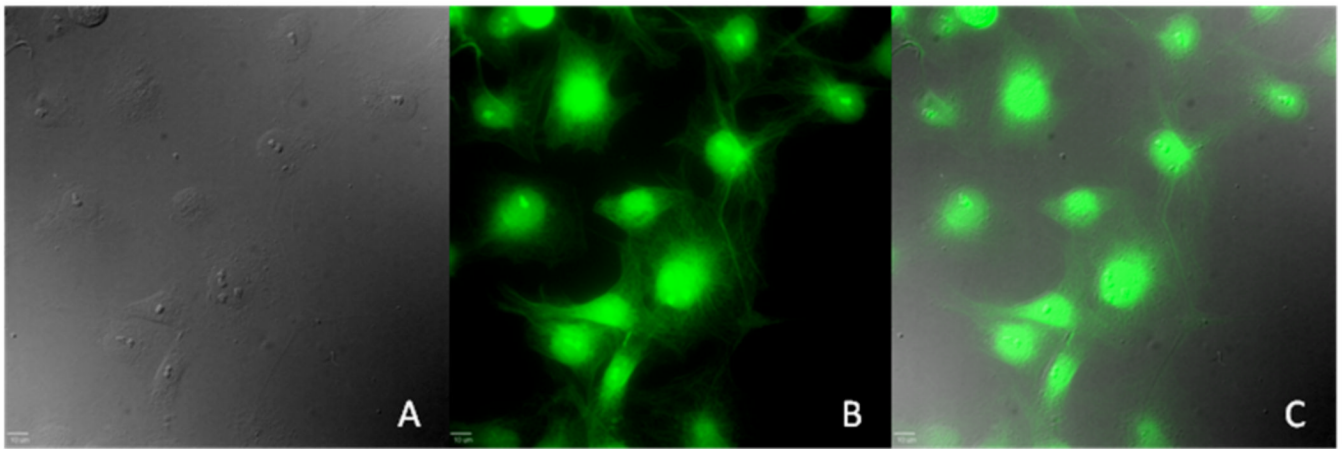

Figure 6.

HeLa cells in PBS media, incubated for 1 h with fluorene-IgG conjugate from a 40 μM solution in PBS buffer; UPlanSApo, N.A.=1.35, 60× oil immersion. A) DIC, 350 ms; B) one-photon fluorescence (Ex: 377/50-DM:409-Em: 525/40), 400 ms; C) overlay of A) and B). Scale bar 10 μm.

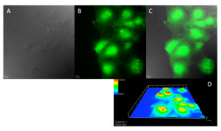

Figure 7.

HeLa cells in PBS media, incubated for 5 h with fluorene-IgG conjugate from a 40 μM solution in PBS buffer; UPlanSApo, N.A.=1.35, 60× oil immersion. A) DIC, 350 ms; B) one-photon fluorescence, (Ex: 377/50-DM:409-Em: 525/40) 450 ms; C) overlay of A and B; D) one-photon fluorescence intensity plot, 450 ms. Scale bar 10 μm.

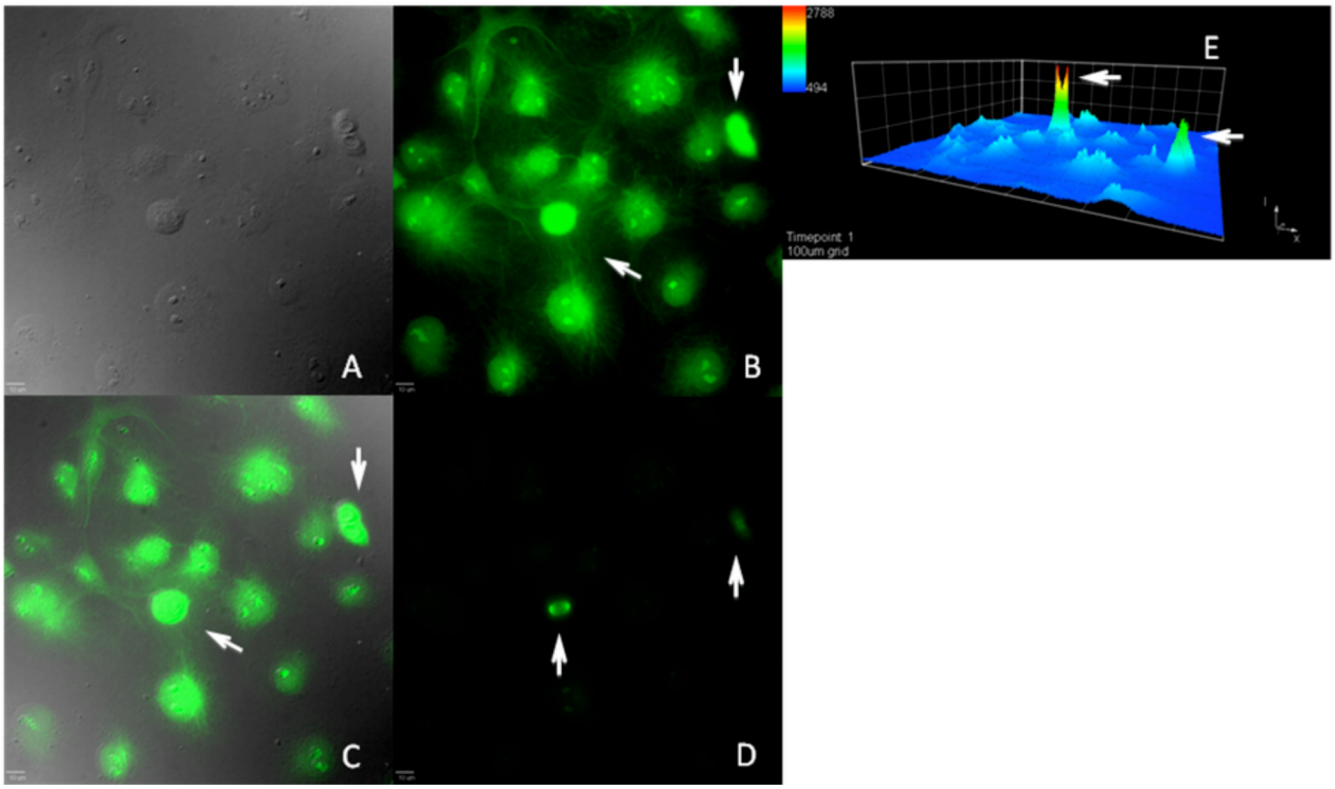

Figure 8.

HeLa cell lines in PBS media, incubated for 5h with fluorene-IgG conjugate from a 40 μM solution in PBS buffer; UPlanSApo, N.A.=1.35, 60× oil immersion. A) DIC, 350 ms; B) one-photon fluorescence (Ex: 377/50-DM:409-Em: 525/40), 350 ms; C) overlay of A and B; D) one-photon fluorescence (Ex: 377/50-DM:409-Em: 525/40), 25 ms; E) one-photon fluorescence intensity graphs, 25 ms. Arrows in B, D, and E show mitotic cells. Scale bar 10 μm.

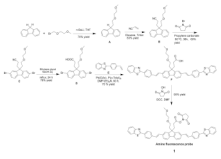

Scheme 1.
Preparation of the succinimidyl amine-reactive tag **1**.

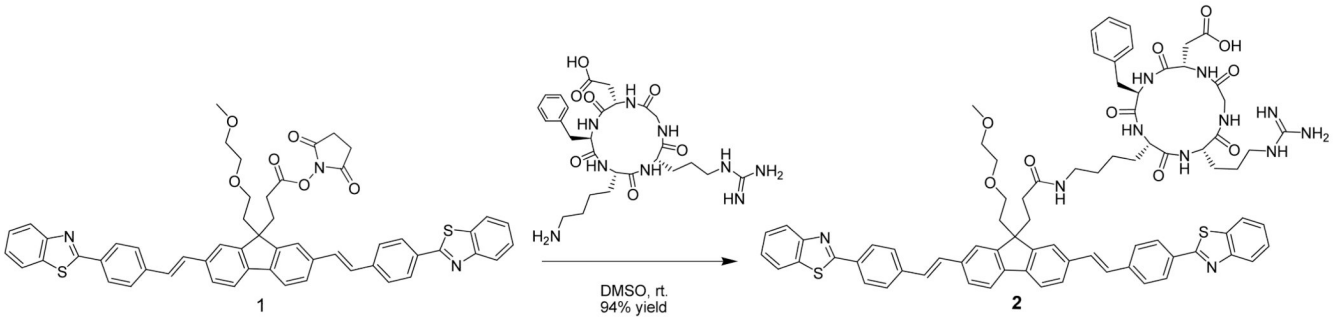

Scheme 2.
Preparation of the fluorene-RGD peptide conjugate **2** with the amine-reactive tag **1**.

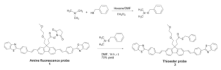

Scheme 3.
Preparation of the thioester probe **3** with the amine-reactive tag **1**.